Penerbit Akademia Baru

Journal of Advanced Research in Fluid Mechanics and Thermal Sciences

Journal homepage: www.akademiabaru.com/arfmts.html
ISSN: 2289-7879

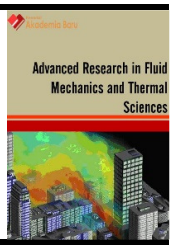

Effects of Wall Thickness on Flame Stabilization Limits for Combustors with Wire Mesh

Open Access

Fudhail Abdul Munir[1,*], Muhmmad Ikhwan Muazzam[1], Abdel Gader[1], Masato Mikami[2], Herman Saputro[3], Laila Fitriana[4]

[1] Faculty of Mechanical Engineering, Universiti Teknikal Malaysia Melaka, Hang Tuah Jaya Melaka, Malaysia
[2] Department of Mechanical Engineering, Graduate School of Science and Engineering, Yamaguchi University, Japan
[3] Department of Mechanical Engineering, Faculty of Education and Teacher Training, Universitas Sebelas Maret, Indonesia
[4] Department of Mathematics Education, Faculty of Education and Teacher Training, Universitas Sebelas Maret, Indonesia

ARTICLE INFO

Article history:
Received 25 March 2018
Received in revised form 6 May 2018
Accepted 22 August 2018
Available online 2 September 2018

Keywords:
Flame stabilization limits, wall thermal conductivity, Computational fluid dynamics (CFD)

ABSTRACT

The scarcity of energy has led to the invention of alternative solutions to the conventional power generators. Micro-power generation system is one of the potential sustainable solutions that provide better energy resource for small electronic devices as compared to conventional lithium-ion batteries. The difficulty to stabilize the flame in micro-combustors is the main obstacle faced by researchers, which is hugely caused from heat loss. Nevertheless, huge efforts towards attaining flame stabilization have been made within this few years back. In this research, the effect of combustor thickness on the flame stabilization limits of micro combustors with stainless steel wire mesh has been investigated. Numerical simulations were performed using a two-dimensional (2-D) and three-dimensional (3-D) steady-state model. The governing equations were solved using ANSYS Release 16.2 with Fluent capability. From the results, it is suggested that the flame stabilization limits for the combustors made of quartz tube has a direct relationship with the wall thickness. Nevertheless, the strategy of improving flame stabilization limits by increasing the wall thickness has a limited range of effectiveness.

1. Introduction

In the present days, electronic gadgets like mobile phones and computer laptops have become must have equipment. With the invention of highly sophisticated electronic devices, the demand for batteries with the capability of greater energy capacity, shorter charging period and lightweight design are skyrocketing. The recent progress in micro power generation systems in which hydrocarbon fuels are utilized might become the viable solution of having a better power source as compared to batteries [1]. Micro power generation system can be defined as a small-scale generation electrical power from heat harvested [2].

* *Corresponding author.*
E-mail address: fudhail@utem.edu.my (Fudhail Abdul Munir)

One of the key components in micro power generation is the narrow channel combustor. It is fundamentally important to understand micro combustion phenomena so that a reliable micro combustor can be designed [3]. Even though flame stabilization in a confined space is reported to be achievable, it is considerably a great challenge to sustain a stable flame such narrow channel. The main reason that contribute to this predicament is mainly due to the high surface to volume ratio [4] that causes a large portion of heat loss from the flame to the wall. As a result, flame quenching occurs within a matter of seconds [5].

Researchers have shown that there are many ways to stabilize flame in a micro combustor. One of the most popular methods is by utilizing the heat produced from the combusted products to pre-heat the unburned reactants. This method is also defined as heat recirculation method. Generally, there are two types of pre-heating method [3]. The first method is called as the direct method where the heat is transferred from the hot burned gas to the unburned gas region through conduction and radiation. Single channel micro combustor (SC) mainly utilizes this type of heat recirculation mechanism in which the heat from the burned gas region is axially transferred to the unburned gas region via the combustor wall [6]. As such, the combustion stability can be significantly enhanced. On the other hand, indirect pre-heating method is an approach where the flow of the burned gas is reversed to pre-heat the unburned reactants. Swiss-roll combustor utilizes this concept resulting to a huge improvement of flame stabilization limits as compared to SC combustors. Nevertheless, the geometry of a Swiss-roll combustor is relatively complicated making it difficult to be numerically and experimentally investigated. Thus, a combustor with simpler geometry is preferred.

Mikami *et al.,* [4] had proposed the use of flame holder in a single channel quartz tube combustor. In their experimental work, a stainless-steel wire mesh is placed between the burned and unburned gas region and the experimental results show that the flame can be stabilized without external heating. Combustion stability in meso and micro-scale combustors is greatly influenced by a few factors such as the wall thickness and materials [7,8]. The effects of wall thermal conductivity on the combustion stability in meso and micro-scale combustors with gaseous hydrocarbon fuels have been thoroughly examined [9,10]. However, these studies are limited to combustors without a flame holder. This research specifically investigated the effect of wall thickness on the flame stabilization limits for micro combustors with stainless steel wire mesh.

2. Methodology

2.1 Governing Equations

The type of fuel used is propane-air mixture while one-step global reaction chemistry is employed. The governing equations utilized for the numerical model are the typical fluid motion combined with reacting flows [11]. The mass conservation equation (continuity) is given by;

$$\frac{\partial \rho}{\partial t} + \frac{\partial}{\partial x}(\rho u_x) + \frac{\partial}{\partial y}(\rho u_y) + \frac{\partial}{\partial z}(\rho u_z) = S_m \tag{1}$$

S_m is the source term. An example of this term is vaporization of liquid or any user-defined source. Nevertheless, in this numerical model the value of S_m is fixed to 0. For a steady state condition, $\frac{\partial \rho}{\partial t} = 0$. The momentum conservation equation in *x*-direction

$$\frac{\partial \rho u_x}{\partial t} + \frac{\partial (\rho u_x u_x)}{\partial x} + \frac{\partial (\rho u_y u_x)}{\partial y} + \frac{\partial (\rho u_z u_x)}{\partial z} = -\frac{\partial p}{\partial x} - \frac{\partial}{\partial x}\left(\frac{2}{3}\mu(\nabla \cdot \vec{u}) + 2\mu \frac{\partial u_x}{\partial x}\right) + \frac{\partial}{\partial y}\left[\mu\left(\frac{\partial u_y}{\partial x} + \frac{\partial u_x}{\partial y}\right)\right] + \frac{\partial}{\partial z}\left[\mu\left(\frac{\partial u_x}{\partial z} + \frac{\partial u_z}{\partial x}\right)\right] + \rho f_x \tag{2}$$

Momentum equation in *y*-direction;

$$\frac{\partial(\rho u_x u_y)}{\partial x}+\frac{\partial(\rho u_y u_y)}{\partial y}+\frac{\partial(\rho u_z u_y)}{\partial z}=-\frac{\partial p}{\partial y}-\frac{\partial}{\partial x}\left[\mu\left(\frac{\partial u_y}{\partial x}+\frac{\partial u_x}{\partial y}\right)\right]+\frac{\partial}{\partial y}\left(\frac{2}{3}\mu(\nabla\cdot\vec{u})+2\mu\frac{\partial u_y}{\partial y}\right)+\frac{\partial}{\partial z}\left[\mu\left(\frac{\partial u_z}{\partial y}+\frac{\partial u_y}{\partial z}\right)\right]+\rho f_y \quad (3)$$

Momentum equation in *z*-direction

$$\frac{\partial(\rho u_x u_z)}{\partial x}+\frac{\partial(\rho u_y u_z)}{\partial y}+\frac{\partial(\rho u_z u_z)}{\partial z}=-\frac{\partial p}{\partial z}-\frac{\partial}{\partial x}\left[\mu\left(\frac{\partial u_x}{\partial z}+\frac{\partial u_z}{\partial x}\right)\right]+\frac{\partial}{\partial y}\left[\mu\left(\frac{\partial u_z}{\partial y}+\frac{\partial u_y}{\partial z}\right)\right]+\frac{\partial}{\partial z}\left(\frac{2}{3}\mu(\nabla\cdot\vec{u})+2\mu\frac{\partial u_y}{\partial z}\right)+\rho f_z \quad (4)$$

where

$$\nabla\cdot\vec{u}=\frac{\partial u_x}{\partial x}+\frac{\partial u_y}{\partial y}+\frac{\partial u_z}{\partial z} \quad (5)$$

The energy transfers due to conduction, species diffusion and viscous dissipation is represented by the Equation (6) and (7) respectively.

$$\nabla\cdot(\vec{u}(\rho E+p))=\nabla\cdot\left(k\nabla\mathrm{T}-\sum_i h_i\vec{J}_i+(\bar{\bar{\tau}}\cdot\vec{u})\right)+S_h \quad (6)$$

$$\nabla\cdot(\vec{u}\rho h)=\nabla\cdot(k\nabla\mathrm{T})+S_h \quad (7)$$

where S_h is heat of chemical reaction or any other volumetric heat sources added by the user. Equation (6) and (7) has already included the pressure work and kinetic energy terms. However, the numerical model is assumed to be incompressible flows and neglects these types of works.
For the species transport equation is defined as:

$$\nabla\cdot(\rho\vec{u}Y_i)=-\nabla\cdot\vec{J}_i+R_i+S_i \quad (8)$$

where R_i and S_i is the net rate of production of species *i* by chemical reaction and rate of creation by addition from the dispersed phase plus any user-defined sources. For the mass diffusion in laminar flows, Fluent employs the dilute approximation, which is also known as Fick's law to model the mass diffusion due to the concentration gradients. The equation for the mass diffusion is given as;

$$\vec{J}_i=-\rho D_{i,m}\nabla Y_i-D_{T,i}\frac{\nabla T}{T} \quad (9)$$

2.2 Boundary Conditions

The boundary treatment at the interface between the fluid and solid wall is assumed to be no-slip boundary type. The heat flux at this interface is calculated using Fourier's law. Heat transfer per unit area by means of convection and radiation at the outer surface of the combustor wall is given as:

$$q_{loss}=h_{conv}(T_{wall}-T_{amb})+\varepsilon\sigma(T_{wall}^4-T_{amb}^4) \quad (10)$$

where h_{conv} is the convective heat transfer coefficient, T_{wall} is the wall temperature of the combustor

and T_{amb} is defined as the ambient temperature. The value of T_{amb} is initialized to 295 K. The value of h_{conv} is fixed to be at constant 5 W/m^{2}K. Since the combustor is assumed to be made of aluminum, the external emissivity (ε) for the outer wall is fixed to 0.31 while value of ε for the wire mesh is set 0.70. The value of Stefan-Boltzmann constant (σ) used is $5.67 \times 10^{-8}\mathrm{W/m^2K^4}$. A thermal insulation (zero heat flux boundary) is applied at both left and right wall edge of the combustor. For the outlet boundary condition, a fixed pressure inlet is applied. A symmetrical boundary condition is established at the origin of z-plane so that the calculation can be performed only in half of the domain. The material thermal properties and the gas transport data are obtained from Fluent internal database [11,12]. Initially, the momentum and continuity equation are solved. Then, the energy and species equations are solved by applying a sufficiently high temperature of 1600 K to the patching zone, which is defined 1 mm from the outlet.

2.3 Blowout Limits Determination

Once ignited, the flame propagates to the upstream and eventually stabilizes near the wire mesh. With a fixed equivalence ratio (ϕ), both blowout and extinction limits are obtained by gradually changing the inlet flow velocity (U). The computational domain for the numerical model is depicted in Figure 1.

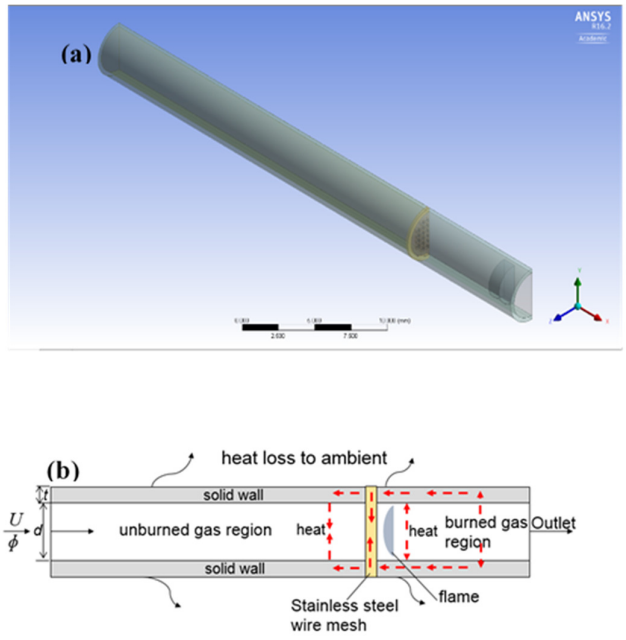

Fig. 1. (a) Computational domain of the three-dimensional numerical model (b) Two-dimensional view of the computational domain

3. Results and Discussion

Figure 2 shows the gas temperature contours for different wall thickness for the combustors with wire mesh. The equivalence ratio is set to 0.90 while the inlet velocity, U is fixed to 0.35 m/s. As seen in the figure, higher wall thickness contributes to the increase of temperature in the unburned gas region.

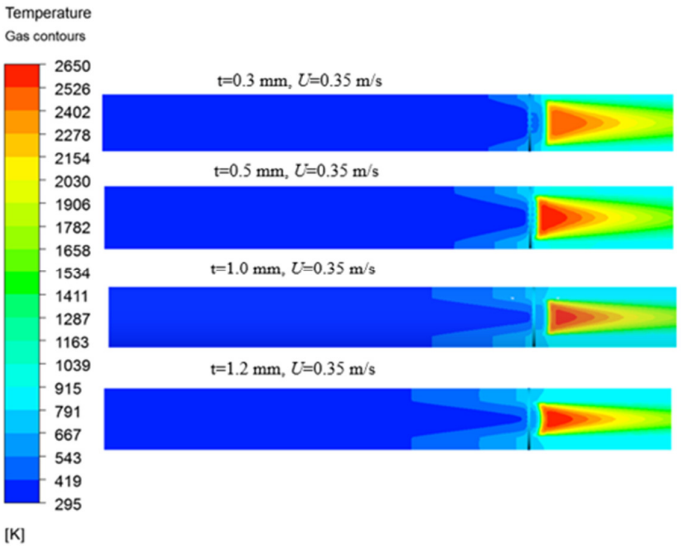

Fig. 2. Gas temperature contour for inlet velocity of U=0.35 m/s for different wall thickness of 0.3, 0.5 mm, 1.0 mm and 1.2 mm respectively

Meanwhile, the heat of reaction rate for each of wall thickness is presented in Figure 3. It can be said that the flame shape is consistent regardless of wall thickness.

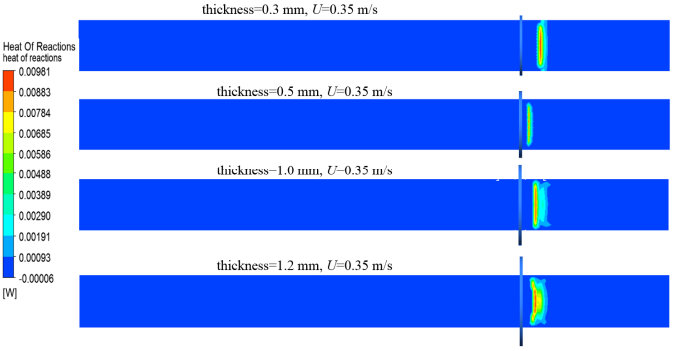

Fig. 3. Heat of reaction for inlet velocity of *U*=0.35 m/s for different wall thickness of 0.3,0.5 mm, 1.0 mm and 1.2 mm respectively

Next, the blowout limits velocity obtained is plotted on the same graph as shown in Figure 4. As suggested from the figure, there is a direct relationship between the blowout limits velocity and the combustors wall thickness. However, as the thickness is further increased from 1.0 mm to 1.2 mm, there is no change of blowout velocity as indicated in the figure.

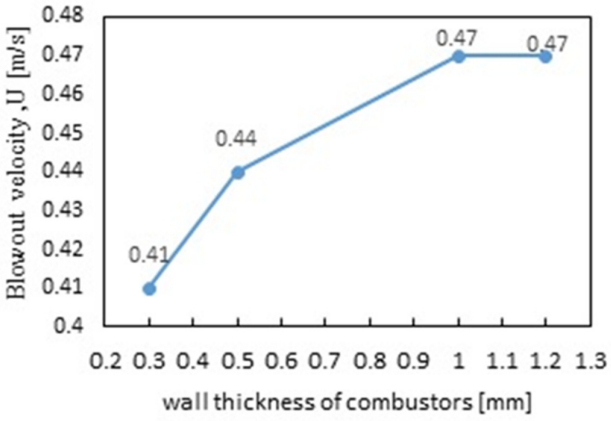

Fig. 4. Relationship between blowout limits and the combustor wall thickness

4. Conclusion

This paper has successfully demonstrated the effect of combustor wall thickness on the flame stabilization limits for combustors with stainless steel wire mesh. It can be deducted that the combustor wall thickness has a direct relationship with the flame stabilization limits for combustors with wall thickness. Nevertheless, the strategy of enhancing blowout limits by modifying the combustor wall thickness is only effective within a certain range.

Acknowledgement

This work partially supported by the seed grant PJP/2016/FKM-CARE/S01505 of Universiti Teknikal Malaysia Melaka.

References

[1] J. Chen, W. Song, and D. Xu, *Energy Convers. Manag.* 134 (2017).
[2] Jiang, Dongyue, Wenming Yang, Kian Jon Chua, and Jianyong Ouyang. "Thermal performance of micro-combustors with baffles for thermophotovoltaic system." *Applied Thermal Engineering* 61, no. 2 (2013): 670-677.
[3] Munir, Fudhail Abdul, and Masato Mikami. "A numerical study of propane-air combustion in meso-scale tube combustors with concentric rings." Journal of Thermal Science and Technology 10, no. 1 (2015): JTST0008-JTST0008.
[4] Mikami, Masato, Yoshiyuki Maeda, Keiichiro Matsui, Takehiko Seo, and Lilis Yuliati. "Combustion of gaseous and liquid fuels in meso-scale tubes with wire mesh." *Proceedings of the Combustion Institute* 34, no. 2 (2013): 3387-3394.
[5] Wan, Jianlong, Aiwu Fan, and Hong Yao. "Effect of the length of a plate flame holder on flame blowout limit in a micro-combustor with preheating channels." *Combustion and Flame*170 (2016): 53-62.
[6] Munir, Fudhail Abdul, Masato Mikami, Muhammad Zahir Hassan, and Mohd Azli Salim. "Flame stabilization in multiple inlet channel meso-scale tube combustors with wire mesh." *Journal of Advanced Vehicle System* 4, no. 1 (2017): 20-27.
[7] Yang, Weijuan, Chen Deng, Junhu Zhou, Jianzhong Liu, Yang Wang, and Kefa Cen. "Experimental and numerical investigations of hydrogen–air premixed combustion in a converging–diverging micro tube." *International Journal of Hydrogen Energy* 39, no. 7 (2014): 3469-3476.
[8] Wenming, Yang, Chou Siawkiang, Shu Chang, Xue Hong, and Li Zhiwang. "Effect of wall thickness of micro-combustor on the performance of micro-thermophotovoltaic power generators." *Sensors and Actuators A: Physical* 119, no. 2 (2005): 441-445.
[9] Kaisare, Niket S., and Dionisios G. Vlachos. "A review on microcombustion: Fundamentals, devices and applications." Progress in Energy and Combustion Science 38, no. 3 (2012): 321-359.

[10] Norton, Dan G., and Dionisios G. Vlachos. "Combustion characteristics and flame stability at the microscale: a CFD study of premixed methane/air mixtures." *Chemical engineering science* 58, no. 21 (2003): 4871-4882.
[11] ANSYS Fluent Release 14.0. In: Inc A, editor. Canonsburg,2012.
[12] Granta's CES EduPack. "Granta Material Intelligence." Granta Design Limited 2007.